Poststroke neuronal rescue and synaptogenesis mediated *in vivo* by protein kinase C in adult brains

Miao-Kun Sun*†‡, Jarin Hongpaisan*†§, Thomas J. Nelson*, and Daniel L. Alkon*

*Blanchette Rockefeller Neuroscience Institute, West Virginia University, Morgantown, WV 26505; and §Laboratory of Neurobiology, National Institute of Neurological Disorders and Stroke, National Institutes of Health, Bethesda, MD 20892

Communicated by Bernhard Witkop, National Institutes of Health, Bethesda, MD, June 20, 2008 (received for review April 28, 2008)

Global cerebral ischemia/hypoxia, as can occur during human stroke, damages brain neural networks and synaptic functions. The recently demonstrated protein kinase C (PKC) activation–induced synaptogenesis in rat hippocampus suggested the potential of PKC-mediated antiapoptosis and synaptogenesis during conditions of neurodegeneration. Consequently, we examined the effects of chronic bryostatin-1, a PKC activator, on the cerebral ischemia/hypoxia–induced impairment of synapses and neurotrophic activity in the hippocampal CA1 area and on hippocampus-dependent spatial learning and memory. Postischemic/hypoxic bryostatin-1 treatment effectively rescued ischemia-induced deficits in synaptogenesis, neurotrophic activity, and spatial learning and memory. These results highlight a neuroprotective signaling pathway, as well as a therapeutic strategy with an extended time window for reducing brain damage due to stroke by activating particular PKC isozymes.

bryostatin | ischemia | neuroprotection | protein kinase C | rat

Temporary or permanent restriction of cerebral blood flow and oxygen supply results in cerebral ischemia and ischemic stroke, the third-leading cause of death and the most common cause of long-term disability in developed countries. Thrombolytic therapy (eg, recombinant tissue plasminogen activator) to achieve early arterial recanalization is the only option currently available to treat ischemic stroke. But this therapy's time-dependent effect (within 3 h after the event) limits its clinical use to only 5% of candidate patients (1), and it carries an increased risk of intracranial hemorrhage, reperfusion injury, and diminishing cerebral artery reactivity (2–5). Neuronal death and injury after cerebral ischemia involve pathological changes associated with necrosis and delayed apoptosis (6, 7). Neurons in the infarction core of focal, severe stroke are immediately eliminated and cannot be saved once ischemia develops. The ischemic penumbra, (i.e, brain tissues surrounding the core in focal ischemic stroke) and the sensitive neurons/networks in global cerebral ischemia are still sustained by the diminished blood supply, however. Further damage in these ischemic brain tissues occurs in a delayed manner after cerebral ischemia/stroke (8–10), responsible for clinical deterioration. Thus, effective postischemic therapy with an extended time window remains one of the greatest challenges to modern medical practice.

A consistent consequence of cerebral ischemia/hypoxia in humans and other mammals is central nervous system dysfunction, the nature of which depends on the location and extent of injury. It has been well established that global cerebral ischemia/hypoxia selectively injures or damages the pyramidal neurons in the dorsal hippocampal CA1 area (11–14), which are essential for episodic memory, providing a sensitive measure for monitoring ischemic damage and recovery functionally. Experimental cerebral ischemia is usually induced focally through, for example, occlusion of the middle cerebral artery, or globally, through permanent occlusion of two arteries (bilateral vertebral arteries in a 4-vessel occlusion model or carotid arteries) associated with a controlled period of occlusion of the other two arteries (bilateral carotid arteries), hypotension, or hypoxia (6, 15). In young adult animals, the combined procedure is essential to induce ischemic pathophysiologic consequences (6, 16–19).

Using confocal and electron microscopy, the potent PKC activator bryostatin was recently shown to enhance precisely those structural and ultrastructural changes in hippocampal synapses specifically affecting rat spatial maze learning and memory (20). Based on that study and other studies (21–24), as well as on previous observations of ischemia/hypoxia-induced damage to CA1 hippocampal neurons (14), we investigated the possibility that bryostatin also may reduce or prevent the aforementioned neuronal and synaptic damage in the postischemic brain.

Results

Global Cerebral Ischemia/Hypoxia Impairs Spatial Learning and Memory. Global cerebral ischemia/hypoxia, induced by permanently occluding the bilateral common carotid arteries, combined with brief hypoxia after complete recovery from the surgery, produced a dramatic and lasting impairment (persisting for at least 6 weeks after the cerebral ischemic/hypoxic event) in spatial learning (ischemia vs. sham-operated: $F_{1,127} = 79.751$, $P < 0.001$; Fig. 1*A*) and memory (ischemic vs. sham-operated: $F_{1,15} = 9.451$, $P < 0.01$; Fig. 1 *B–F*) in young adult Wistar rats. This global cerebral ischemic/hypoxic model is particularly relevant to clinical situations involving restriction of both oxygen and blood flow, such as cardiac arrest, coronary bypass surgery, and neurovascular surgeries.

Bryostatin-1 Activates PKC. Instead of intervening in the pathological process that already has occurred in the ischemic brain (25, 26), we used bryostatin-1 (21, 27), a potent PKC activator with an antitumorigenic pharmacologic profile, in an attempt to boost neurorepair activity and synaptogenesis pharmacologically. Bryostatin-1, which crosses the blood-brain barrier when administered peripherally (28), produces a relatively selective activation of the PKCε isozyme, which is neuroprotective (29–31) and has a lower median effective dose than PKCδ for bryostatin-1 in its translocation (thus activation), whereas PKCδ is most likely involved in ischemic injury during ischemia-reperfusion (32–34). We recently showed that PKC activation with bryostatin-1 enhanced exactly those synaptogenesis, presynaptic/postsynaptic ultrastructural specialization, and protein synthesis functions involved in rat maze learning and memory (20, 35). PKC activation has at least two actions that may be relevant to PKC signal processing: activation of PKC isozymes at low concentrations and protection of active, membrane-bound PKC from degradation under stress. In cultured rat hippocampal IGF1R cells, bryostatin-1 at 0.2 nM activated PKC, with a maximal effect (about twofold) at 30 min (Fig. 2*A*). Higher concentrations produced briefer activation. In addition, under cellular stress, the loss of nutrients and growth factors, as mimicked by serum deprivation, PKC isozyme levels in the cultured rat hippocampal IGF/IR cells decreased dramatically (Fig. 2*B*). By

Author contributions: M.-K.S., J.H., T.J.N., and D.L.A. designed research; M.-K.S., J.H., and T.J.N. performed research; M.-K.S. and J.H. analyzed data; and M.-K.S., J.H., T.J.N., and D.L.A. wrote the paper.

The authors declare no conflict of interest.

†M.-K.S. and J.H. contributed equally to this work.

‡To whom correspondence should be addressed. E-mail: mksun@brni-jhu.org.

© 2008 by The National Academy of Sciences of the USA

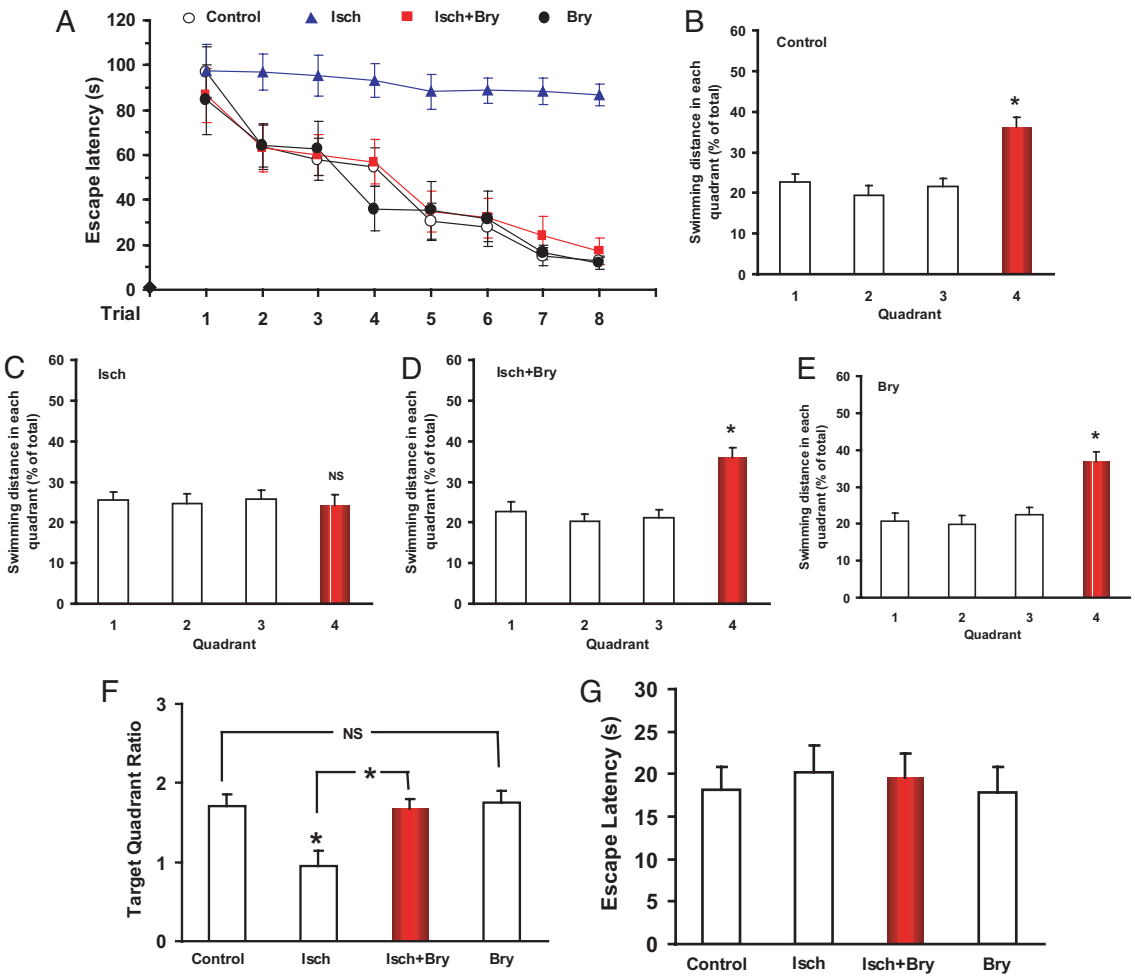

Fig. 1. Chronic bryostatin-1 rescued rats' performance in spatial learning and memory but did not affect their sensorimotor ability. (*A*) Escape latency over training trials (mean ± standard error of the mean). (*B–E*) Results of the memory retention test after the training trials. Quadrant 4 was the target quadrant where the hidden platform was placed during the training trials. (*F*) Target quadrant ratio (calculated by dividing the target quadrant swim distance by the average swim distance in the nontarget quadrants). (*G*) Results in a visible platform test (with a visible platform placed at a new location). Bry, bryostatin-1; Isch, cerebral ischemia; NS, not significant; *, $P < 0.05$.

96 h, membrane levels of PKCα, PKCδ, and PKCε became almost undetectable, but no changes in the levels of other proteins, including ERK1/2, GSK-3β, and TACE, and total proteins (not shown) were seen. Bryostatin-1 protected preferentially against the down-regulation of the active, membrane-bound PKC isozymes induced by serum deprivation. Membrane PKCα, PKCδ, and PKCε levels were increased by 400%, 350%, and 250%, respectively, above their corresponding control levels (Fig. 2 *C–E*). In contrast, bryostatin-1 had no protective effect on cytosolic PKC (not shown).

Bryostatin-1 Rescues Spatial Learning and Memory After Global Cerebral Ischemia/Hypoxia. Postischemic chronic bryostatin-1 treatment (a 5-week treatment, with the first dose given 24 h after the ischemic/hypoxic event) effectively restored rats' performance in the spatial learning and memory task. Overall, there was a significant difference between the groups ($F_{3,255} = 31.856$; $P < 0.001$; Fig. 1) and groups x trials ($F_{21,255} = 1.648$; $P < 0.05$). The ischemic learning impairment was restored by bryostatin-1 (bryostatin-1+ischemia vs. ischemia: $F_{1,127} = 50.233$; $P < 0.001$), whereas bryostatin-1 alone did not affect the learning (bryostatin-1 vs. sham-operated: $F_{1,127} = 2.258$; $P > 0.05$) when learning capacity was measured 2 weeks after the last bryostatin-1 dose. Thus, the observed differences in learning index capacities were not contaminated by any direct action of bryostatin-1 on learning. In the memory retention test, the sham-operated rats exhibited a target quadrant preference, but the ischemic rats did not demonstrate any measurable memory retention. Bryostatin-1 therapy effectively rescued memory retention after cerebral ischemia to the level of the sham-operated rats, whereas it had no significant effects on the target quadrant preference compared with that of the sham-operated control rats. There was a significant difference in the target quadrant ratios ($F_{3,31} = 6.181$; $P < 0.005$; Fig. 1*F*) between the groups. Detailed analysis of the memory retention test further revealed significant differences between the ischemic rats and ischemic rats with bryostatin-1 treatment ($F_{1,15} = 10.328$; $P < 0.01$), but no significant differences between the ischemic rats with bryostatin-1 treatment and sham-operated control rats ($F_{1,15} = 0.0131$; $P > 0.05$) or between the sham-operated control rats and the bryostatin-1–alone rats ($F_{1,15} = 0.161$; $P > 0.05$).

In separate groups of rats, coadministration of PKC isozyme inhibitor Ro-31–8220 [0.5 mg/kg through a tail vein (22)] significantly attenuated the function-restoring effects of bryostatin-1 on the ischemic impairments of the learning (ischemia+bryostatin-1 vs. ischemia+Ro-31–8220+bryostatin-1: $F_{1,127} = 9.429$; $P < 0.005$) and memory (ischemia+bryostatin-1 vs. ischemia+Ro-31–8220+bryostatin-1: $F_{1,15} = 4.923$; $P < 0.05$; not shown), indicating involvement of PKC activation. Ro-31–8220 alone affected neither the ischemic impairments of learning ($F_{1,127} = 0.282$; $P > 0.05$) nor

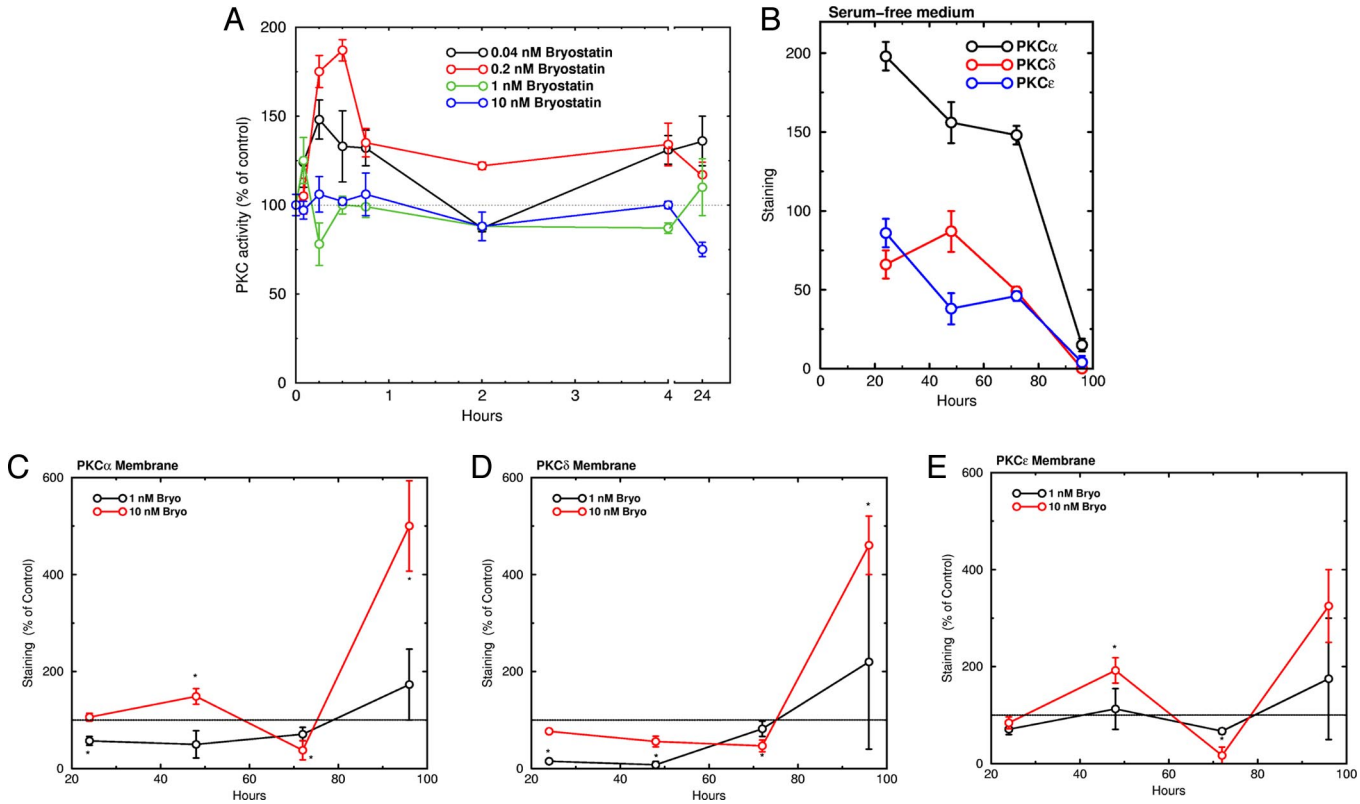

Fig. 2. Bryostatin-1 activated PKC isozymes and protected membrane-associated PKC isozymes from serum deprivation-induced down-regulation in cultured rat hippocampal IGF/IR cells. (*A*) Time course of bryostatin-1 effect on PKC activity. (*B*) Time course of effect of serum deprivation on membrane-associated PKC levels. (*C–E*) Effects of bryostatin-1 on membrane-associated PKC levels under serum deprivation. PKC was measured by Western blot assay and is plotted as percentage of the control value at each time point.

ischemic impairment of memory ($F_{1,15} = 0.0162$; $P > 0.05$) compared with the sham-operated controls. Thus, Ro-31–8220 treatment had no function-restoring effects on spatial learning and memory after the global ischemic injury, but it did significantly attenuate the effects of bryostatin-1 on the learning and memory.

Cerebral Ischemia and Bryostatin-1 Do Not Alter Rats' Sensorimotor Ability. At the end of the probe test, the sensorimotor ability and motivation differences of the rats were tested in a visible platform test. This test involved one trial in each rat to determine whether there were any visual and motor disability and motivation differences that might affect rats' performance in the spatial learning and memory task. Sensorimotor ability and motivation were not affected by the ischemic procedure and bryostatin-1 treatment ($F_{6,55} = 0.218$; $P > 0.05$; Fig. 1*G*) in the visible platform test.

Bryostatin-1 Enhances Neurotrophic Activity and Neuronal Survival After Cerebral Ischemia. The cerebral ischemic/hypoxic event produced significant neural and synaptic damage in the dorsal hippocampal CA1 area, damage that was rescued by chronic bryostatin-1 administration. First, cerebral ischemia reduced the number of surviving pyramidal cells in the hippocampal CA1. There was a significant difference in the number of the surviving cells between the ischemic and sham-operated control rats ($F_{1,11} = 28.938$; $P < 0.001$) and between the ischemia and ischemia with bryostatin-1 treatment ($F_{1,11} = 11.491$; $P < 0.001$; Fig. 3*A*). On the other hand, bryostatin-1 alone did not significantly affect the number of surviving cells in the hippocampal CA1 compared with the control ($F_{1,11} = 0.797$. $P > 0.05$).

Second, bryostatin-1 significantly enhanced the brain-derived neurotrophic factor (BDNF) activity in the dorsal hippocampal CA1 area, a response consistent with the previous observation that elevated BDNF activity in the brain protects neurons against ischemic injury (36, 37). Significant overall differences in BDNF fluorescent intensities of the pyramidal neurons in hippocampal CA1 area were seen in the experimental groups in terms of cell bodies ($F_{5,624} = 39.738$; $P < 0.001$) and dendrites ($F_{5,179} = 9.490$; $P < 0.001$; Fig. 3*B*). In both cell bodies and dendrites, cerebral ischemia increased BDNF levels compared with the levels in the control rats. Bryostatin-1 treatment in the ischemic rats further enhanced the BDNF activity (bryostatin-1+ischemia vs. ischemia: $P < 0.001$ for the cell bodies and $P < 0.05$ for dendrites; Fig. 3*B*). Bryostatin-1 alone also increased BDNF activity compared with the control rats.

Bryostatin-1 Prevents Synaptic Loss and Induces Synaptogenesis After Cerebral Ischemia. Bryostatin-1 rescued an ischemia-induced decrease in dendritic spines and presynaptic vesicles. In the ischemic animals, the number of (postsynaptic) dendritic spines (as measured using the dendritic spine marker spinophilin) was significantly decreased compared with that in the sham-operated control rats (Fig. 3*C*). The number of dendritic spines in the animals treated with bryostatin-1 and ischemia was significantly higher than that in the rats subjected to cerebral ischemia without the bryostatin-1 treatment and in the sham-operated control rats ($P < 0.001$). Bryostain-1 alone also increased the number of dendritic spines compared with that in the control rats. In contrast to the dendritic spines, the number of presynaptic axon boutons (as assayed by the number of synaptophysin granules) were stable and were not affected by global cerebral ischemia and/or chronic bryostatin-1 (Fig. 3*C*). However, the number of presynaptic vesicles, as indexed by synaptophysin intensity, in the axon boutons was changed in a way identical to the alteration of dendritic spines.

Bryostatin-1 rescued the cerebral ischemia-induced loss of mush-

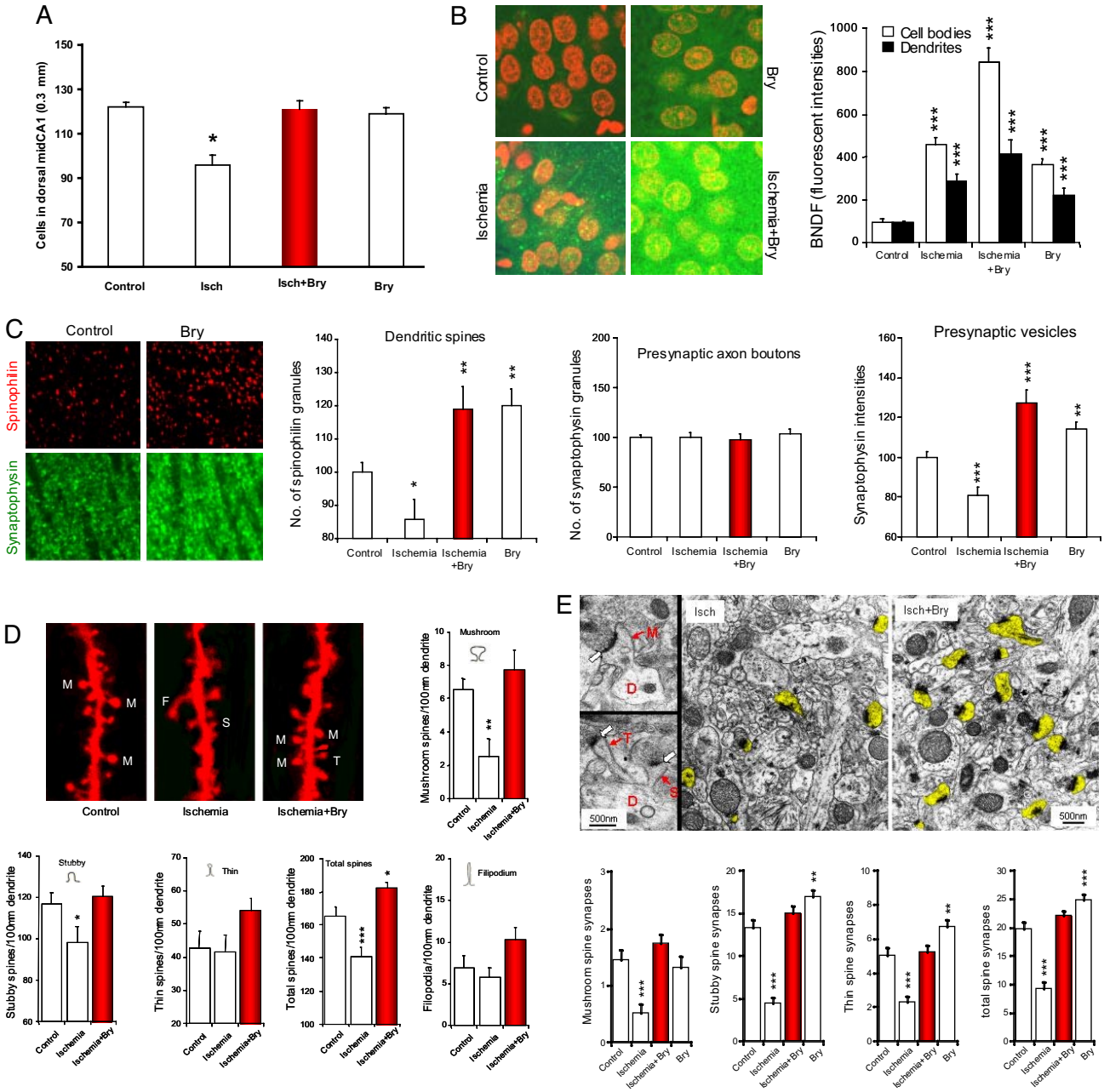

Fig. 3. Chronic bryostatin-1 rescued pyramidal cells, neurotrophic activity, synaptic strength in the dorsal hippocampal CA1 area from cerebral ischemia-induced damage (9 days after the last bryostatin-1 dose of a 5-week treatment and ≈7 weeks after the cerebral ischemic/hypoxic event). (*A*) Effects of cerebral ischemia and bryostatin-1 treatment on the number of surviving cells in the dorsal hippocampal CA1 area. (*B*) Scanning confocal microscopy of BDNF immunohistochemistry (green) in the stratum pyramidale of hippocampal CA1 area. Neuronal nuclei were counterstained by 4′,6-diamdino-2-phenyllindole (red). Cerebral ischemia: $n = 3$ rats, $n = 84$ cell bodies, $n = 30$ dendrite regions. Control: $n = 3$ rats, $n = 123$ cell bodies, $n = 30$ dendrite regions. Ischemia+bryostatin-1: $n = 3$ rats, $n = 99$ cell bodies, $n = 30$ dendrite regions. Bryostatin-1 alone: $n = 3$ rats, $n = 117$ cell bodies, $n = 30$ dendrite regions. (*C*) Scanning confocal microscopy of the stratum radiatum of the hippocampal CA1 areas, studied with the dendritic spine marker spinophilin and the presynaptic vesicle membrane marker synaptophysin. Ischemic: $n = 3$ rats, $n = 28$ random CA1 area. Sham-operated: $n = 5$ rats, $n = 50$ CA1 area. Ischemia+bryostatin-1: $n = 3$ rats, $n = 30$ CA1 area. Bryostain-1 alone: $n = 3$ rats, $n = 30$ CA1 images. (*D*) Changes in different shapes of dendritic spines in stratum radiatum of the hippocampal CA1 area, studied with Dil-staining and imaged by confocal microscopy (M, mushroom spine; S, stubby spine; T, thin spine; F, filopodium). Ischemia: $n = 3$ rats, $n = 16$ dendrites. Sham-operated: $n = 3$ rats, $n = 28$ dendrites. Ischemia+bryostatin-1: $n = 3$ rats, $n = 28$ dendrites. (*E*) Changes in axo-spinous synapses in stratum radiatum of the hippocampal CA1 area. The left-side electron micrographs show the ultrastructures of mushroom (M), stubby (S), and thin (T) spines, branching from the dendritic shaft (D). The heads of these dendritic spines form synapses (white arrows) with presynaptic axonal boutons (A) that contain presynaptic vesicles. Right electron micrographs show the densities of dendritic spines (yellow highlight) in cerebral ischemia with and without bryostatin-1. The bottom panel shows quantification of the different types of and total number of synapses observed. Cerebral ischemia: $n = 3$ rats, $n = 62$ random CA1 area. Sham-operated: $n = 3$ rats, $n = 62$ CA1 area. Ischemia+bryostatin-1: $n = 3$ rats, $n = 61$ CA1 area. Bryostatin-1 alone: $n = 3$ rats, $n = 48$ CA1 area. Bry, bryostatin-1; Isch, cerebral ischemia.

room spine formation. The numbers of mushroom and stubby spines in the animals subjected to ischemia were significantly lower than those in the sham-operated control animals (Fig. 3*D*). Chronic bryostatin-1 restored the numbers of mushroom and stubby spines in the ischemic animals. When the numbers of mushroom, stubby, and thin spines were added together (i.e., the total number of

spines), bryostatin-1 was seen to not only rescue the ischemia-induced loss of dendritic spines, but also to increase the total number of spines compared with that in the sham-operated control animals (Fig. 3*D*), confirming the results of the total number of dendritic spines studied with the dendritic spine marker spinophilin (Fig. 3*C*).

Furthermore, bryostatin-1 prevented the cerebral ischemia–induced loss of dendritic spine synapses. Double-blind analysis and electron microscopy were used to study changes in the numbers of synapses in mushroom, stubby, and thin spines (Fig. 3*E*, white arrows). Cerebral ischemia decreased and chronic bryostatin-1 reversed the numbers of axo-spinous synapses in mushroom, stubby, and thin spines, compared with those in the sham-operated control rats. In summary, the effects of cerebral ischemia on synapse numbers were rescued by chronic bryostatin-1 administration.

Discussion

Global cerebral ischemia/hypoxia administered to rats produced significant damage to the dorsal hippocampal CA1 field and impaired spatial learning and memory that depends on the rat dorsal hippocampus. The results reported here indicate that PKC activation by chronic administration of bryostatin-1 after ischemia with an extended time window (24 h) can improve learning and memory by preventing neuronal loss and maintaining/restoring the dendritic spines and their synapses. Even compared with controls, bryostatin-1 alone significantly increased the numbers of mushroom, stubby, and thin spine synapses (Fig. 3*E*). The mechanisms by which bryostatin-1 restores the numbers of non-mushroom spines include antiapoptosis, synaptogenesis, and spinogenesis. These results using a therapy with an extended time window differ from those obtained from various other strategies that block the pathological cascades that most likely have already caused significant damage by the time treatment begins. It remains to be determined to what degree the postischemic/hypoxic therapeutic effects observed with bryostatin result from promoting neuronal survival/repair, neurogenesis/migration, and/or synaptogenesis. The doses administered in the rats in the present study were within the dose range known to be well tolerated in humans. Within this dose range, adverse reactions in humans are rare and generally mild, and most frequently involve myalgia and/or fatigue. Nevertheless, these therapeutic results may lead to a new drug treatment involving neural repair and restoration that can complement existing thrombolytic therapies by ameliorating and/or preventing post-cerebral ischemia/stroke damage to synaptic and neural networks in affected brain regions.

Materials and Methods

Animals, Cerebral Ischemia/Hypoxia, and Drug Treatments. Adult Wistar rats (male, 225–250 g) were housed in a temperature-controlled (20–24°C) room for at least 1 week before experimentation, allowed free access to food and water, and kept on a 12-h light/dark cycle. They were randomly assigned to different groups (8–10 each). Global cerebral ischemia was induced *in vivo* by the two-artery occlusion (2-VO) method, combined with a controlled period of hypoxia (14 min in a jar). The bilateral common carotid arteries (from the ventral side of the neck) were tied with silk threads, under an appropriate level of pentobarbital anesthesia (60 mg/kg intraperitoneally, with additional supplemental doses when necessary). The 2-VO occlusion led to a chronic reduction in cerebral blood flow to 70% of the original flow rate in these young rats. Rectal temperature was monitored throughout the surgery and maintained at 37.5°C, using a heat lamp.

At the end of surgery and under appropriate anesthesia, the rats received ketoprofen (5 mg/kg subcutaneously) for postsurgical pain relief, along with 5 ml of saline to compensate for loss of water and minerals. A 7-day recovery period from surgery was allowed before the period of hypoxic exposure (≈14 min in a jar with blowing in low oxygen of ≈5%). The combined cerebral ischemia/hypoxia resulted in a loss of righting reflex for ≈10 min. Control rats were subjected to an identical procedure, except that the arteries were not occluded and the oxygen level was not reduced in the same jar.

Bryostatin-1 (15 $\mu g/m^2$) and/or Ro-31–8220 (0.5 mg/kg) was administered through a tail vein (2 doses/week, for 10 doses), starting 24 h after the end of the ischemic/hypoxic event. The ability of the rats in spatial learning (2 trials/day for 4 days) and memory (a probe test of 1 min, 24 h after the last trial) was evaluated as the functional endpoint, with the first training started 9 days after the last dose of bryostatin-1 or Ro-31–8220. The delay between the last bryostatin-1/Ro-31–8220 dose and the first spatial maze training trial appears appropriate for a separation of the acute memory action of bryostatin-1 and Ro-31–8220 from their effects on neurorepairing after cerebral ischemia.

All procedures were conducted according to National Institutes of Health Animal Care and Use Committee guidelines, and were approved by the Ethical Committee of the Institute.

Spatial Learning and Memory. Water maze acquisition was used in this study because it was most closely associated with functions of the dorsal hippocampal CA1 pyramidal cells. Rats were moved to the test room in their home cages at least 1 h before daily trials. The maze pool had a diameter of 152 cm and height of 60 cm and was filled with 40 cm H_2O (22 ± 1°C). The maze was divided into four quadrants. Rats were trained for 4 days (2 trials/day) to find a hidden platform (9-cm diameter), centered in one of the quadrants and submerged ≈2 cm below the water surface. At the start of all trials, rats were placed individually in the water facing the maze wall, using different starting positions each trial, and allowed to swim until they found the platform, where they remained for 20 s before being returned to their home cages. A rat that failed to find the platform within 2 min was guided there by the investigator, with 120 s scored. The swim path was recorded with a video-tracking system that computed latency to the platform, swim distance, and percentage of time spent in the quadrants. After the training trials, a probe trial (a quadrant test or retention trial) was given with the platform removed to assess memory retention for its location by the distance the rat moved in the quadrants. The video-tracking system tracked the animal's movements in each quadrant for 1 min.

Visible Platform Test. After completion of the spatial memory procedure, all rats were tested on a visible platform task (with the platform marked with a pole that protruded 9 inches above the water surface but at a new location) to evaluate their sensorimotor abilities and escape-finding motivation differences.

Surviving Cells. At the end of behavioral testing, some rats were perfused transcardially under deep terminal pentobarbital anesthesia with 400 ml of 4% paraformaldehyde. The brains were extracted and postfixed overnight in 4% paraformaldehyde. Coronal 7-mm sections were cut with a rotary microtome. Serial sections through the hippocampal formation were mounted on slides and processed for cresyl violet staining. For counting, a 300-μm-long frame was placed along the mid-CA1 cell layer of the dorsal hippocampus without bias. Cells were counted within the frame, unless they overlapped the top or right side of the frame. Any cell damage was noted.

PKC Activity. Rat hippocampal IGF1R cells (ATCC) in six-well plates were treated with bryostatin-1, then washed with PBS, scraped, and homogenized by sonication in 10 mM Tris-HCl buffer (pH 7.4) containing 50 mM NaF, 1 mg/ml of leupeptin, and 1 mM PMSF. PKC activity was measured enzymatically using incorporation of ^{32}P from $\gamma[^{32}]$ATP into histones in the presence of 300 μg/ml of phosphatidylserine and 45 μg/ml of diacylglycerol (1,2-dioctanoyl-sn-glycerol).

In a separate experiment, rat hippocampal IGF1R cells were incubated in serum-free medium for up to 96 h after treatment with bryostatin-1. The cells were washed, scraped, and homogenized. Cytosol and membrane were separated by centrifugation at 100,000 × *g*. Membrane and cytosolic PKCα, PKCδ, and PKCε protein levels were measured in Western blots by densitometry using IMAL software.

Confocal Microscopy Studies. Changes of BDNF, presynaptic axon boutons, and postsynaptic dendritic spines were studied by confocal microscopy. Under anesthesia (pentobarbital, 80 mg/kg body weight, administered intraperitoneally), rats were perfused through the left cardiac ventricle with phosphate-buffered saline (PBS) at room temperature by gravity to wash out the blood, and then lightly fixed with ≈150 ml of 4% paraformaldehyde in PBS at room temperature, instead of a cold fixative, because hypothermia could reduce the number of dendritic spines. Brains were removed and postfixed for 10 min. Then hippocampi were dissected from the right brain hemispheres, and dorsal hippocampi were sectioned with a vibratome at 400 mm for 1,1′-dioctadecyl-3,3,3′,3′-tetramathylindocarbocyanine perchlorate (DiI) staining and immunohistochemistry.

DiI Staining. Dendritic spines were visualized with DiI (Molecular Probes/Invitrogen), as previously described in ref. 20. Dendritic spines stained with DiI (568 nm/>510 nm; excitation/emission) in stratum radiatum were imaged with a Zeiss Axiovert 200M microscope equipped with 510 confocal scanning system, using a 63× Plan-APO Chromat oil immersion objective (1.4 NA). Confocal images

(512 × 512 pixels) were collected with line scan mode and a pinhole of ≈1.00 Airy unit. A stack of confocal images (taken every 0.45 μm) was collected to obtain all dendritic spines of an individual dendritic shaft.

During analysis, a stack of images was retrieved with the Image J program (http://rsb.info.nih.gov/ij/). Individual spines identified on one image were also verified on adjacent stacked images to approximate the three-dimensional structure of this spine. Those spines, which had head diameters more than three times larger than the diameter of their necks and appear in more than three planes of the stacked images, were identified as mushroom spines. About four to six stacked image sets were obtained from each animal. All image sets were pooled and coded; therefore, images were identified with unknown animal number and unknown treatment (double-blind protocol).

Immunohistochemistry. Immunohistochemistry was modified from our previous study (*27*). Hippocampal slices at 35-μm thickness were incubated free-floating with primary antibodies against BDNF (monoclonal IgG, 1:50; Santa Cruz Biotechnology), the dendritic spine marker spinophilin (polyclonal IgG, 1:100;/Upstate/Millipore), and the presynaptic vesicle membrane protein synaptophysin (monoclonal IgG; 1:2,000; Chemicon/Millipore), in PBS containing 0.1% Triton X-100 and 15% horse serum in PBS at room temperature overnight. Sections were then incubated for 3 h at room temperature with the following secondary antibodies: Alexa Fluor 568 goat anti-rabbit IgG (1: 200; Molecular Probes) for spinophilin, and biotinylated horse anti-mouse antibody (1:20; Vector Labs) for BDNF and synaptophysin. Tissue sections, incubated with biotinylated secondary antibodies, were then incubated with streptavidin conjugated with Alexa Fluor 488 (1: 100; Molecular Probes) for 3 h at room temperature. After Alexa staining, all sections were mounted on glass slides with Vectashield mounting medium with 4′,6-diamidino-2-phenylindole (Vector Labs) to counterstain nuclei and sealed with cover glasses.

Hippocampal slices were imaged with the above confocal microscope setting (only single plane image/area) and quantified by the Image J program. The expression of BDNF in the cell bodies of the hippocampal CA1 neurons, counterstained nuclei with 4′,6-diamidino-2-phenylindole, was determined at a single cell level from fluorescent intensities of BDNF in CA1 stratum pyramidale. The expression of BDNF in dendrites was defined by measuring the overall fluorescent intensities of BDNF in confocal images (63 μm × 63 μm) of the superficial part of stratum radiatum. The appearance of spinophilin and synaptophysin profiles in a 63 μm × 63 μm image, taken from the superficial part of stratum radiatum, was analyzed with the photographic negative after background subtraction. The total numbers of dendritic spines (spinophilin granules) and presynaptic axon boutons (synaptophysin granules) were then counted. The volume of presynaptic vesicles was evaluated from the fluorescent intensity of synaptophysin. The control data were set at 100%, and all other experiment data were defined at percentage of their control.

Electron Microscopy Studies. Ultrastructures of presynaptic, axonal boutons, postsynaptic dendritic spines, and their synapses were studied by electron microscopy, as described previously (27). Rats that had been anesthetized with choral hydrate were perfused through the heart with 2% glutaradehyde and 3% paraformadehyde. Removed brains were postfixed with the same fixative at 4°C overnight. Then the right dorsal hippocampi were sectioned with a vibratome to 100 μm. Hippocampal slices were washed three times with cacodylate buffer (pH 7.4), postfixed in 1% OsO4 for 1 h, and then rinsed with distilled water. The slices were dehydrated in a graded ethanol series, followed by resin embedding and then sectioning using standard procedures. Ultra-thin sections (90 nm) were stained with uranyl acetate and lead acetate and viewed at 100 kV in a JEOL 200CX electron microscope. During double-blind quantification, electron micrographs (100 μm^2 CA1 area at 5000×) were digitally zoomed up to 20,000× magnification using the Preview program on an iMac G5 computer with an Mac OS X operating system and a 19-inch monitor. Spines were defined as structures that formed synapses with axon boutons and contained no mitochondria. Quantitative classification of dendritic spines as mushroom spines required that either spine ''heads'' attached to a clearly distinguishable ''neck'' had a cross-sectionally visualized diameter > 600 nm, measured by the Image J program, or spine ''heads'' not attached to a clearly distinguishable neck had (cross-sectionally visualized) both long and short axis lengths > 600 nm.

Statistical analysis was performed using analysis of variance, followed by the Newman-Keuls multiple-comparisons test, or using the Student *t* test for paired and unpaired data wherever appropriate. A P value < 0.05 was considered significant.

1. Hossmann KA (2006) Pathophysiology and therapy of experimental stroke. *Cell Mol Neurobiol* 26:1057–1083.
2. Cipolla MJ, Lessov N, Clark WM, Haley EC Jr (2000) Postischemic attenuation of cerebral artery reactivity is increased in the presence of tissue plasminogen activator. *Stroke* 31:940–945.
3. Cocho D, *et al.* (2005) Reasons for exclusion from thrombolytic therapy following acute ischemic stroke. *Neurology* 64:719–720.
4. Wang J, Tsirka SE (2005) Contribution of extracellular proteolysis and microglia to intracerebral hemorrhage. *Neurocrit Care* 3:77–85.
5. Gonzalez RG (2006) Imaging-guided acute ischemic stroke therapy: From ''time is brain'' to ''physiology is brain.'' *AJNR Am J Neuroradiol* 27:728–735.
6. Lipton P (1999) Ischemic cell death in brain neurons. *Physiol Rev* 79:1431–1568.
7. Reitz C, Bos MJ, Hofman A, Koudstaal PJ, Breteler MB (2008) Prestroke cognitive performance, incident stroke, and risk of dementia: The Rotterdam Study. *Stroke* 39:36–41.
8. Hara K, *et al.* (2007) Prestroke cognitive performance, incident stroke, and risk of dementia: The Rotterdam Study. *Brain Res Bull* 74:164–171.
9. Lee S-R, *et al.* (2007) Reduction of hippocampal cell death and proteolytic responses in tissue plasminogen activator knockout mice after transient global cerebral ischemia. *Neuroscience* 150:50–57.
10. Sallustio F, Diomedi M, Centonze D, Stanzione O (2007) Saving the ischemic penumbra: Potential role for statins and phosphodiesterase inhibitors. *Curr Vasc Pharmacol* 5:259–265.
11. Kirino T (1982) Delayed neuronal death in the gerbil hippocampus following ischemia. *Brain Res* 239:57–69.
12. Pulsinelli WA, Brierley JB, Plum F (1982) Temporal profile of neuronal damage in a model of transient forebrain ischemia. *Ann Neurol* 11:491–498.
13. Nakatomi H, *et al.* (2002) Regeneration of hippocampal pyramidal neurons after ischemic brain injury by recruitment of endogenous neural progenitors. *Cell* 110:429–441.
14. Bendel O, *et al.* (2005) Reappearance of hippocampal CA1 neurons after ischemia is associated with recovery of learning and memory. *J Cereb Blood Flow Metab* 25:1586–1595.
15. Olson EE, McKeon RJ (2004) Characterization of cellular and neurological damage following unilateral hypoxia/ischemia. *J Neurol Sci* 227:7–19.
16. Sun M-K, Alkon DL (2004) Cerebral hypoperfusion and amyloid-induced impairment of hippocampal CA1 synaptic efficacy and spatial memory in young adult rats. *J Alzheimers Dis* 6:355–366.
17. de la Torre JC, Stefano GB (2000) Evidence that Alzheimer's disease is a microvascular disorder: The role of constitutive nitric oxide. *Brain Res Brain Res Rev* 34:119–136.
18. Farkas E, Luiten PGM (2001) Cerebral microvascular pathology in aging and Alzheimer's disease. *Prog Neurobiol* 64:575–611.
19. Kalaria RN (2000) The role of cerebral ischemia in Alzheimer's disease. *Neurobiol Aging* 21:321–330.
20. Hongpaisan J, Alkon DL (2007) A structural basis for enhancement of long-term associative memory in single dendritic spines regulated by PKC. *Proc Natl Acad Sci U S A* 104:19571–19576.
21. Alkon DL, Sun M-K, Nelson TJ (2007) PKC signaling deficits: A mechanistic hypothesis for the origins of Alzheimer's disease. *Trends Pharmacol Sci* 28:51–60.
22. Pascale A, Govoni S, Battaini F (1998) Age-related alteration of PKC, a key enzyme in memory processes: Physiological and pathological examples. *Mol Neurobiol* 16:49–62.
23. Bell KF, Zheng L, Fahrenholz F, Cuello AC (2008) ADAM-10 overexpression increases cortical synaptogenesis. *Neurobiol Aging* 29:554–565.
24. Sun M-K, Alkon DL (2006) Bryostatin-1: Pharmacology and therapeutic potential as a CNS drug. *CNS Drug Rev* 12:1–8.
25. Grotta JC (1999) Acute stroke therapy at the millennium: Consummating the marriage between the laboratory and bedside. The Feinberg lecture. *Stroke* 30:1722–1728.
26. Gladstone DJ, Black SE, Hakim AM (2002) Toward wisdom from failure: Lessons from neuroprotective stroke trials and new therapeutic directions. *Stroke* 33:2123–2136.
27. Hennings H, *et al.* (1987) Bryostatin 1, an activator of protein kinase C, inhibits tumor promotion by phorbol esters in SENCAR mouse skin. *Carcinogenesis* 8:1343–1346.
28. Zhang X, *et al.* (1996) Preclinical pharmacology of the natural product anticancer agent bryostatin 1, an activator of protein kinase C. *Cancer Res* 56:802–808.
29. Jia J, *et al.* (2007) Activations of nPKCepsilon and ERK1/2 were involved in oxygen-glucose deprivation–induced neuroprotection via NMDA receptors in hippocampal slices of mice. *J Neurosurg Anesthesiol* 19:18–24.
30. Raval AP, Dave KR, Mochly-Rosen D, Sick TJ, Pérez-Pinzón MA (2003) Epsilon PKC is required for the induction of tolerance by ischemic and NMDA-mediated preconditioning in the organotypic hippocampal slice. *J Neurosci* 23:384–391.
31. Lange-Asschenfeldt C, *et al.* (2004) Epsilon protein kinase C–mediated ischemic tolerance requires activation of the extracellular-regulated kinase pathway in the organotypic hippocampal slice. *J Cereb Blood Flow Metab* 24:636–645.
32. Chou WH, Messing RO (2005) Protein kinase C isozymes in stroke. *Trends Cardiovasc Med* 15:47–51.
33. Bright R, *et al.* (2005) Protein kinase C delta mediates cerebral reperfusion injury *in vivo*. *J Neurosci* 24:6880–6888.
34. Bright R, Steinberg GK, Mochly-Rosen D (2007) Delta PKC mediates microcerebrovascular dysfunction in acute ischemia and in chronic hypertensive stress *in vivo*. *Brain Res* 1144:146–155.
35. Alkon DL, Epstein H, Kuzirian A, Bennett MC, Nelson TJ (2005) Protein synthesis required for long-term memory is induced by PKC activation on days before associative learning. *Proc Natl Acad Sci U S A* 102:16432–16437.
36. Nomura T, *et al.* (2005) I.V. infusion of brain-derived neurotrophic factor gene–modified human mesenchymal stem cells protects against injury in a cerebral ischemia model in adult rat. *Neuroscience* 136:161–169.
37. Zhang Y, Pardridge WM (2006) Blood-brain barrier targeting of BDNF improves motor function in rats with middle cerebral artery occlusion. *Brain Res* 1111:227–229.